ELSEVIER

Sensors and Actuators A 50 (1995) 151–156

SENSORS AND ACTUATORS A PHYSICAL

Fabrication and dynamic testing of electrostatic actuators with p^+ silicon diaphragms

E.H. Yang, S.S. Yang *, S.W. Han, S.Y. Kim

Microsystems Laboratory, Department of Control and Instrumentation Engineering, Ajou University, 5 Wonchun-Dong, Suwon, 442-749, South Korea

Received 7 June 1995; accepted in revised form 15 September 1995

Abstract

This paper presents the fabrication and testing of electrostatic actuators with p^+ diaphragms. The actuators consist of two counter electrodes which are fabricated on a silicon wafer and Pyrex glass, respectively. The p^+ diaphragm is used as a moving electrode, whereas the aluminium layer deposited on #7740 Pyrex glass is used as a fixed electrode. According to the calculation of static deflection of diaphragms with residual tensile stress, corrugated diaphragms deflect more than a flat one in most deflection regions. The dynamic characteristics of an actuator with a corrugated diaphragm and one with a flat diaphragm are tested and compared with the calculation results.

Keywords: Corrugated diaphragms; p^+ Diaphragms; Residual stress; Electrostatic actuators; Dynamic testing

1. Introduction

During recent years, microelectromechanical systems have been used for a variety of applications. Among these applications, microactuators as the elements of micropumps have been widely studied [1–18]. There are several principles for the actuation of micropumps, such as piezoelectric [1–4], thermopneumatic [5–9], electrohydrodynamic [10,11], electrostatic [12–16] and electrochemical actuation [17]. The electrostatic actuator has the advantages of no temperature dependence and simplicity of fabrication over other actuators. The application of electrostatic actuators to micropumps have been experimentally studied by some researchers [13,16,18]. In general, the electrostatic actuator is driven by the electrostatic attraction force between two parallel plates. In this paper, we consider a p^+ silicon diaphragm as a movable electrode of the actuator. The p^+ silicon film is simply fabricated by the boron-doped chemical etch-stop method, which is useful for the fabrication of microsensors and microactuators. However, the residual stress distribution in the p^+ film degrades the performance of the actuator. The residual tensile stress reduces the deflection of a flat diaphragm with pressure, while the residual compressive stress causes buckling [19–21].

One way to solve these problems is to fabricate a corrugated diaphragm for stress release [22]. If no residual stress exists, a corrugated diaphragm deflects more than a flat one in the large-deflection region, and vice versa in the small-deflection region [23–26]. If the residual stress is not negligible, the diaphragm behaviour is different from those with no residual stress. While a flat diaphragm deflects less due to residual tensile stress, a corrugated diaphragm is not so much affected by residual stress. For large corrugation depth, the diaphragm deflection is almost equal to that of a stress-free diaphragm [23]. Thus, the deflection of a corrugated diaphragm can be larger than that of a flat one in the small-deflection region under sufficient residual tensile stress. For the electrostatic actuator application, however, large corrugation may not be desirable because the attraction force of the electrostatic actuator is inversely proportional to the square of the distance between two electrodes.

The static characteristics of corrugated and flat diaphragms under residual tensile stress have been investigated [17,23], but a dynamic test by electrostatic actuation has not yet been performed. In this paper, an electrostatic actuator with a corrugated diaphragm and another with a flat one have been fabricated. Their dynamic characteristics are tested and compared with the calculation results of static deflection under residual tensile stress. Finally, it is to be determined which diaphragm is preferable for electrostatic actuation under residual tensile stress.

* Corresponding author.

SSDI0924-4247(95)01042-6

2. Deflection by electrostatic actuation

Figs. 1 and 2 illustrate schematic views of an actuator with a corrugated p^+ diaphragm and of another with a flat diaphragm, respectively. The p^+ diaphragms are moving electrodes and an aluminium layer deposited on #7740 Pyrex glass is the fixed electrode. In these Figures d_1 is the initial air gap of the electrodes, d_2 is the thickness of the insulation layer, h is the thickness of the diaphragm, H is the corrugation depth and l is the spatial period of corrugation.

When a voltage is applied to the counter electrodes of the actuators, an electrostatic force is generated between the electrodes. The actuator diaphragms are deflected by the attraction force. For the actuator with a flat diaphragm, the electrostatic force, F, is

$$F=\frac{1}{2}\left[\frac{\epsilon_2(d_1-y)}{\epsilon_2(d_1-y)+\epsilon_1 d_2}\right]^2 \epsilon_1 V^2 \frac{A}{(d_1-y)^2} \tag{1}$$

where A is the area of the electrode and ϵ_1 and ϵ_2 are the permittivities of air and the insulator, respectively. V is the potential difference between the electrodes. In the case of a corrugated diaphragm, it is impossible to derive analytically

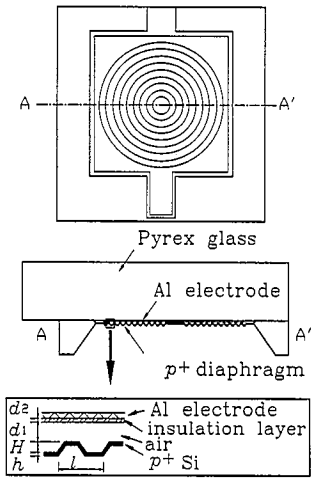

Fig. 1. Schematic view of the electrostatic actuator with a corrugated diaphragm.

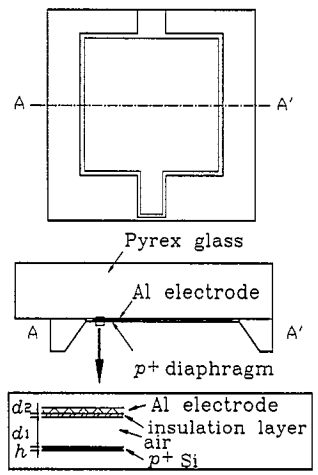

Fig. 2. Schematic view of the electrostatic actuator with a flat diaphragm.

the electrostatic force between the corrugated electrode and the flat one. For an approximate estimation of the force, the electrodes are regarded as being parallel with an equivalent air gap. The equivalent air gap is determined by calculating the average of the distance between the aluminium layer and the corrugation profile of the diaphragm.

When one side of a diaphragm with radius a is exposed to some pressure, the approximate relationship between the applied force, F, and the static centre deflection of the flat diaphragm, y, under the residual stress σ_r is given by [23]

$$F=4hy\left[\sigma_r+\frac{2.83}{4}\frac{E}{(1-\nu^2)}\frac{y^2}{a^2}\right] \tag{2}$$

where E and ν are Young's modulus and Poisson's ratio, respectively. The relationship between the applied force and the static deflection of the corrugated diaphragm under residual stress is [23]

$$F=4hy\left[\sigma_r\frac{B_p}{2.83}+\frac{A_p}{4}E\frac{h^2}{a^2}\right] \tag{3}$$

A_p and B_p are

$$A_p=\frac{2(q+3)(q+1)}{3[1-(\nu/q)^2]}$$

$$B_p=32\frac{(1-\nu^2)}{(q^2-9)}\left[\frac{1}{6}-\frac{3-\nu}{(q-\nu)(q+3)}\right] \tag{4}$$

where q is the corrugation quality factor representing the corrugation geometry. For a sinusoidal corrugation profile, q is defined as

$$q^2=\frac{s}{l}\left[1+1.5\left(\frac{H}{h}\right)^2\right] \tag{5}$$

where s is the corrugation arc length. Fig. 3 shows typical force–deflection curves of a flat diaphragm. The dimensions of the diaphragm are arbitrarily set to $h=3.5$ μm and $a=1500$ μm (see Table 1). The electrode gaps are $d_2=0.3$ μm and $d_1=20$ μm. Fig. 3 illustrates two kinds of curves. One represents the electrostatic force of Eq. (1) when 55 V is applied between the electrodes. The others represent the deflection of the diaphragm with residual stress. The intersection of two curves means the equilibrium point of static deflection. Fig. 4 shows the static centre deflection of a diaphragm with resid-

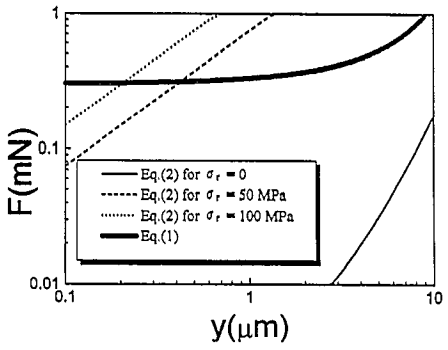

Fig. 3. Centre deflection of flat diaphragm vs. electrostatic force.

Table 1
The dimensional parameters of the actuators

Parameter	Corrugated (μm)	Flat (μm)
a	1500	1500
h	3.5	2
d_1	20	10
d_2	0.3	0.3
l	60	
s	74	
H	14	

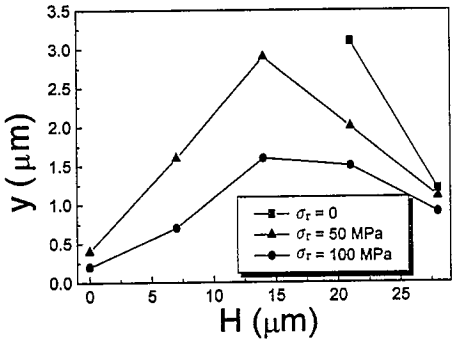

Fig. 4. Static centre deflection of diaphragm with residual stress for various corrugation depths.

ual stress for various corrugation depths obtained from Eqs. (1) and (2) when 55 V is applied. As the corrugation becomes large, the effect of the residual stress decreases. Most p^+ silicon films have residual tensile stress of 40–100 MPa [19–21,26–28]. From Fig. 4, it is obvious that in the case of a corrugated diaphragm with residual stress above 50 MPa, a diaphragm with a corrugation depth of 14 μm has the largest deflection.

A corrugated diaphragm with $H=14$ μm has been fabricated, and the expected deflection is about 2 μm. For comparison, another actuator having a flat diaphragm with $h=2$ μm and $d_1=10$ μm has been fabricated.

3. Fabrication

Fig. 5 shows the fabrication process of the actuators. The starting material is a double-side polished n-type (100) silicon wafer 450 μm thick. Initially, 0.8 μm thick oxide is thermally grown for an etch mask. For the fabrication of the space between the two counter electrodes, the frontside of the wafer is etched with EPW solution by 20 μm in the case of a corrugated diaphragm, and by 10 μm for a flat one. After the residual oxide is etched off, 0.5 μm thick thermal oxide is grown again. In order to fabricate the corrugated diaphragm, the silicon wafer is patterned and etched by 14 μm with KOH to form concentric corrugations, whereas the wafer for the flat one is not etched. To make references for alignment, the wafer is etched through with EPW etchant. Boron is diffused into the corrugated and flat surfaces to make p^+ etch-stop layers. The diffusion is performed with a BN1100 solid source in N_2 ambient gas at 1100 °C for 10 h. After removal of the BSG layer, a drive-in process for 1 h at 1000 °C is followed by patterning for the backside etch of the wafer. The backside of the water is etched with EPW to fabricate the diaphragms. In the case of the flat diaphragm, the surface of the p^+ layer of the frontside is etched for 30 min to avoid the possibility of buckling of the diaphragm. Fig. 6(a) shows an SEM photograph of the cross section of a corrugated p^+

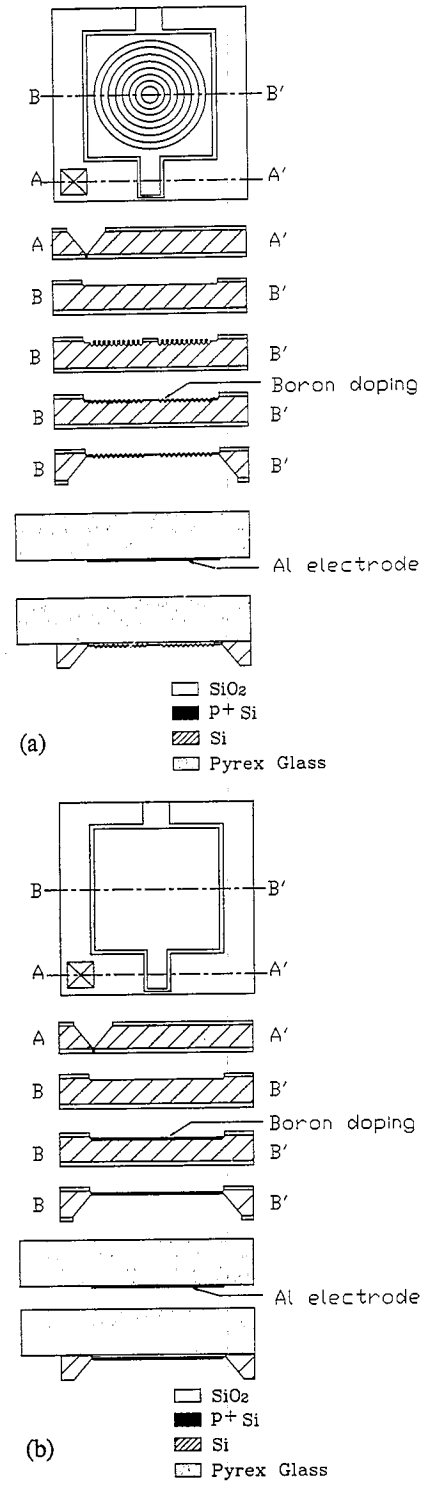

Fig. 5. Fabrication process: (a) corrugated type; (b) flat type.

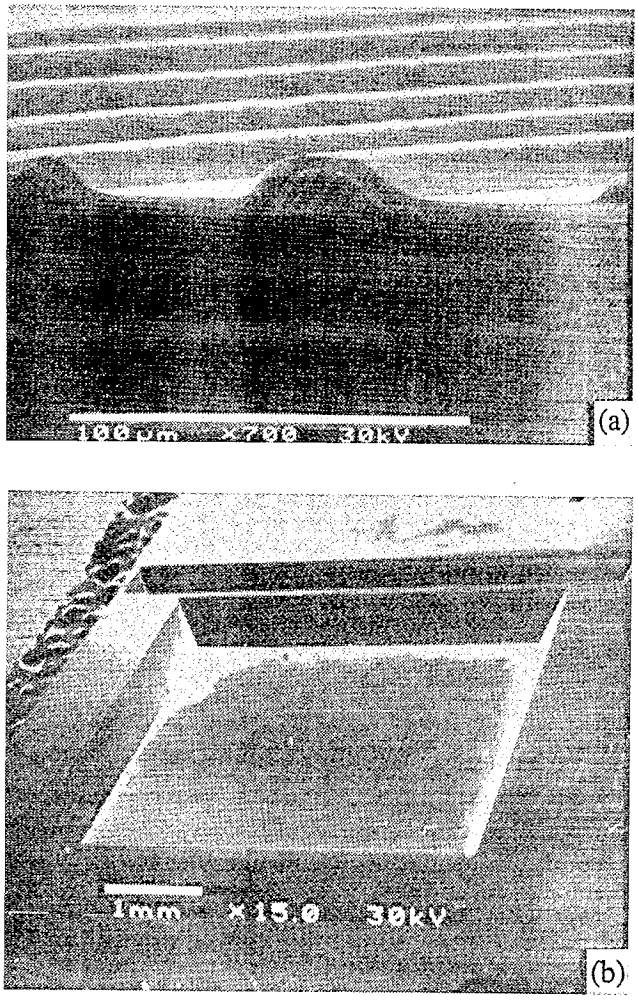

Fig. 6. SEM photographs of diaphragms: (a) cross section of a corrugated diaphragm; (b) backside of a flat diaphragm.

diaphragm. An SEM photograph of the backside of a flat p^+ diaphragm is shown in Fig. 6(b). In order to construct the counter electrodes, the processed silicon wafer is anodically bonded with #7740 Pyrex glass on which an aluminium electrode is deposited. The anodic bonding is performed at 300 °C with 800 V applied. During the bonding, the space between the two electrodes is not sealed to prevent the diaphragm from swelling due to the expansion of gas in the cavity. Since the thermal expansion coefficient of Pyrex glass [29] is close to that of silicon [30], the thermal stress after bonding is negligibly small compared to the residual stress of p^+ silicon.

4. Experiments and discussion

The dynamic characteristics of the fabricated actuators are obtained by measuring the velocity of the centre of the diaphragm using a laser vibrometer (Polytec OFV352 sensor head with OFV2600 controller). The output signal is integrated to get the displacement signal using an FFT analyser (Lecroy 9310 dual oscilloscope). An a.c. sinusoidal voltage is applied between the two electrodes with varying frequency.

Fig. 7 illustrates the measured frequency response of the corrugated diaphragm for an input voltage of 55 V. The static deflection estimated from the experimental result is about 0.2 μm. As shown in Fig. 4, the static deflection of the corrugated diaphragm under a tensile stress of 100 MPa is expected to be 1.6 μm. The difference between the measured and the calculated value is mainly due to the error in calculating the electrostatic force generated between the corrugated and the flat electrodes. In this paper, the electrostatic force is approximately calculated as the force generated between two flat electrodes assuming that a virtual flat electrode instead of the corrugated diaphragm is located at the centre of the corrugation. Accurate calculation of the electrostatic force between the corrugated diaphragm and the flat electrode is beyond the scope of this paper.

Fig. 8 illustrates the measured frequency response of the flat diaphragm for an input voltage of 50 V. The static deflection estimated from the experimental result is about 1.5 μm. Based on the calculation of Eqs. (1) and (2), the fabricated flat diaphragm is expected to deflect by 1.9 μm under a tensile stress of 100 MPA when 50 V is applied. The measured deflection of the flat diaphragm is close to the calculated value. In the case of the flat p^+ diaphragm, the shallow etch of the p^+ layer surface prevents the diaphragm from buckling, since the surface subjected to compressive residual stress is removed. However, the overall residual stress in the diaphragm becomes more tensile and the deflection of the diaphragm reduces. From the results, it is confirmed that the corrugated diaphragm is not adequate for electrostatic actuation and the flat one is preferable.

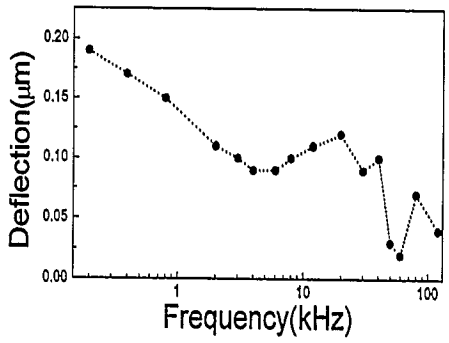

Fig. 7. Measured frequency response of corrugated diaphragm.

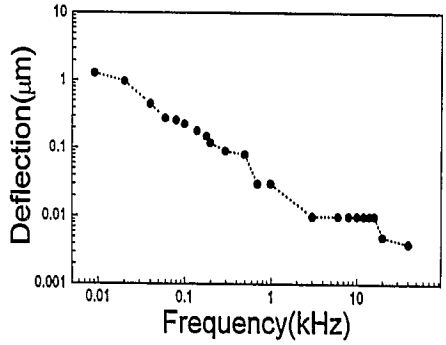

Fig. 8. Measured frequency response of flat diaphragm.

5. Conclusions

Two electrostatic actuators with p^+ diaphragms as moving electrodes have been fabricated, and a dynamic test by electrostatic actuation has been performed. One actuator has a corrugated diaphragm and the other a flat diaphragm. According to the calculation, the corrugated diaphragm deflects more than the flat one when residual tensile stress exists in the diaphragm. This is because the residual stress of the diaphragm is released to some extent by the corrugation. The test results illustrate that the deflection of the corrugated diaphragm is much less than that estimated approximately, but that the flat diaphragm deflects almost as estimated. This is mainly due to the error in calculating the electrostatic force generated between the corrugated and the flat electrode. This result means that a corrugated diaphragm has no advantage over a flat one in electrostatic applications because of its geometrical limitation.

References

[1] J.G. Smits, Piezoelectric micropump with three valves working peristaltically, *Sensors and Actuators, A21–A23* (1990) 203–206.

[2] W. Tjhen, T. Tamagawa, C.P. Ye, C.C. Hsueh, P. Schiller and D.L. Polla, Properties of piezoelectric thin films for micromechanical devices and systems, *IEEE Microelectromech. Systems Workshop, Nara, Japan, 30 Jan.–2 Feb., 1991*, pp. 114–119.

[3] E. Stemme and G. Stemme, A novel piezoelectric valve-less fluid pump, *Tech. Digest, 7th Int. Conf. Solid-State Sensors and Actuators, (Transducers '93), Yokohama, Japan, 7–10 June, 1993*, pp. 110–113.

[4] T. Gerlach and H. Wurmus, Working principle and performance of the dynamic micropump, *IEEE Microelectromech. Systems Workshop, Amsterdam, The Netherlands, 29 Jan.–2 Feb., 1995*, pp. 221–226.

[5] B. Büstgens, W. Bacher, W. Menz and W.K. Schomburg, Micropump manufactured by thermoplastic molding, *IEEE Microelectromech. Systems Workshop, Oiso, Japan, 25–28 Jan., 1994*, pp. 18–21.

[6] J.A. Folta, N.F. Raley and E.W. Hee, Design, fabrication and testing of a miniature peristaltic membrane pump, *IEEE Solid-State Sensor and Actuator Workshop, Hilton Head Island, SC, USA, 22–25 June, 1992*, pp. 186–189.

[7] F.C. Pol, H.T.G. Lintel, M. Elwenspoek and J.H.J. Fluitman, A thermopneumatic micropump based on micro-engineering techniques, *Sensors and Actuators, A21–A23* (1990) 198–202.

[8] F.C. Pol, D.G.J. Wonnik, M. Elwenspoek and J.H.J. Fluitman, A thermo-pneumatic actuation principle for a microminiature pump and other micromechanical devices, *Sensors and Actuators, 17* (1989) 139–143.

[9] T.S.J. Lammerink, M. Elwenspoek and J.H.J. Fluitman, Integrated micro-liquid dosing systems, *IEEE Microelectromech. Systems Workshop, Fort Lauderdale, FL, USA, 7–10 Feb., 1993*, pp. 254–259.

[10] A. Richter, A. Plettner, K.A. Hofmann and H. Sandmaier, Electrohydrodynamic pumping and flow measurement, *IEEE Microelectromech. Systems Workshop, Nara, Japan, 30 Jan.–2 Feb., 1991*, pp. 271–276.

[11] G. Fuhr, R. Hagendorn, T. Müller, W. Benecke and B. Wagner, Pumping of water solution in microfabricated electrohydrodynamic system, *IEEE Microelectromech. Systems Workshop, Travemünde, Germany, 4–7 Feb., 1992*, pp. 26–30.

[12] J. Branebjerg and P. Gravesen, A new electrostatic actuator providing improved stroke length and force, *IEEE Microelectromech. Systems Workshop, Travemünde, Germany, 4–7 Feb., 1992*, pp. 6–11.

[13] R. Zengerle, A. Richter and H. Sandmaier, A micro membrane pump with electrostatic actuation, *IEEE Microelectromech. Systems Workshop, Travemünde, Germany, 4–7 Feb., 1992*, pp. 19–24.

[14] R. Zengerle, M. Richter, F. Brosinger, A. Richter and H. Sandmaier, Performance simulation of micromachined membrane pumps, *Tech. Digest, 7th Int. Conf. Solid-State Sensors and Actuators (Transducers '93), Yokohama, Japan, 7–10 June, 1993*, pp. 106–109.

[15] J.K. Robertson and K.D. Wise, A nested electrostatically-actuated microvalve for an integrated microflow controller, *IEEE Microelectromech. Systems Workshop, Oiso, Japan, 25–29 Jan., 1994*, pp. 7–12.

[16] R. Zengerle, S. Kluge, M. Richter and A. Richter, A bidirectional silicon micropump, *IEEE Microelectromech. Systems Workshop, Amsterdam, The Netherlands, 29 Jan.–2 Feb., 1995*, pp. 19–24.

[17] M.W. Hamberg, C. Neagu, J.G.E. Gardeniers, D.J.I. Jntema and M. Elwenspoek, An electrochemical micro actuator, *IEEE Microelectromech. Systems Workshop, Amsterdam, The Netherlands, 29 Jan.–2 Feb., 1995*, pp. 106–110.

[18] S.S. Yang, E.H. Yang, S.Y. Kim, J.D. Seo and S.H. Yoo, Fabrication of an electrostatic actuator and passive valves with p^+ diaphragms for micropumps, *ASME Winter Annual Meet., DSC-55-2, Chicago, IL, USA, 6–10 Nov., 1994*, pp. 733–740.

[19] F. Maseeh and S.D. Senturia, Plastic deformation of highly doped silicon, *Sensors and Actuators, A21–A23* (1990) 861–865.

[20] X. Ding, W.H. Ko and J.M. Mansour, Residual stress and mechanical properties of boron-doped p^+ silicon films, *Sensors and Actuators, A21–A23* (1990) 866–871.

[21] X. Ding and W.H. Ko, Buckling behavior of boron doped p^+ silicon diaphragms, *Tech. Digest, 6th Int. Conf. Solid-State Sensors and Actuators (Transducers '91), San Francisco, CA, USA, 24–28 June, 1991*, pp. 93–96.

[22] V.L. Spiering, S. Bouwstra, R.M.E.J. Spiering and M. Elwenspoek, On-chip decoupling zone for package-stress reduction, *Tech. Digest, 6th Int. Conf. Solid-State Sensors and Actuators (Transducers '91), San Francisco, CA, USA, 24—28 June, 1991*, pp. 982–985.

[23] P.R. Scheeper, W. Olthuis and P. Bergveld, The design, fabrication, and testing of corrugated silicon nitride diaphragms, *J. Microelectromech. Syst., 3* (1994) 36–42.

[24] J.H. Jerman, The fabrication and use of micromachined corrugated silicon diaphragms, *Sensors and Actuators, A21–A23* (1990) 988–992.

[25] C.J. Mullem, K.J. Gabriel and H. Fujita, Large deflection performance of surface micromachined corrugated diaphragms, *Tech. Digest, 6th Int. Conf. Solid-State Sensors and Actuators (Transducers '91), San Francisco, CA, USA, 24–28 June, 1991*, p. 1014–1017.

[26] Y. Zhang and K.D. Wise, Performance of non-planar silicon diaphragms under large deflections, *IEEE Microelectromech. Systems Workshop, Fort Lauderdale, FL, USA, 7–10 Feb., 1993*, pp. 284–288.

[27] E.H. Yang and S.S. Yang, The quantitative determination of the residual stress profile in oxidized p^+ silicon films, *Sensors and Actuators A*, submitted for publication.

[28] L.B. Wilner, Strain and strain relief in highly doped silicon, *IEEE Solid-State Sensor and Actuator Workshop, Hilton Head Island, SC, USA, 22–25 June, 1992*, pp. 76–77.

[29] K.E. Petersen, Silicon as a mechanical material, *Proc. IEEE, 70* (1982) 420.

[30] L. Meites, *Handbook of Analytical Chemistry*, McGraw-Hill, New York, 1st edn, 1963, Ch. 3, p. 238.

Biographies

Eui Hyeok Yang was born in Korea in 1967. He received his B.S. and M.S. degrees in control and instrumentation engineering from Ajou University in 1990 and 1992, respec-

tively. He is currently working towards his Ph.D. degree in the field of microelectromechanical systems at Ajou University. His research interests include the mechanism, actuation and fabrication of microsensors and microactuators.

Sang Sik Yang was born in Korea in 1958. He received his B.S. and M.S. degrees in mechanical engineering from Seoul National University in 1980 and 1983, respectively. In 1988, he received his Ph.D. degree in mechanical engineering from University of California, Berkeley. He was then a research assistant professor at New Jersey Institute of Technology. Since 1989, he has been an associate professor in the Department of Control and Instrumentation Engineering at Ajou University. His research interests include the mechanism and actuation of microelectromechanical devices, motion control and non-linear control.

Sang Woo Han received his degree in control and instrumentation engineering from Ajou University, Suwon, Korea, in 1995. He is now with Daewoo Heavy Industry.

Seong Yoon Kim received his M.S. degree in control and instrumentation engineering from Ajou University, Suwon, Korea, in 1994. He is now with Daewoo Motors Co., Ltd.